Toumpanaki, E., & Ramage, M. (2019). Bond performance of glued-in CFRP and GFRP rods in timber. In R. Görlacher (Ed.), *INTER : International Network on Timber Engineering Research* (pp. 177-194). (Proceedings). Timber Scientific Publishing.

Peer reviewed version

Bond performance of glued-in CFRP and GFRP rods in timber

Dr. Eleni Toumpanaki, Research Associate, Centre for Natural Material Innovation, University of Cambridge, 1-5 Scroope Terrace, CB2 1PX, email: et343@cam.ac.uk (corresponding author)

Dr. Michael H. Ramage, Senior Lecturer in Architectural Engineering, Director Centre for Natural Material Innovation, Department of Architecture, University of Cambridge, Cambridge, UK

Keywords: Glued-in rods, Bond strength, Engineered timber, Fibre Reinforced Polymer (FRP)

1 Introduction

A rapid growth in multi-storey and tall timber buildings[1] has been observed in the last decade (e.g. the Treet building in Bergen, Norway (14 storeys, 49 m, in 2015) and the Mjøstårnet building in Oslo, Norway (18 storeys, 80 m, in 2018)) heating the competition to build taller with wood with future building proposals (e.g. the River Beech tower (Sanner et al. 2017)) showing tremendous ambition. This growth is the outcome of recent advances in engineered timber, such as glued laminated timber (glulam) and laminated veneer lumber (LVL), the turn towards sustainable building materials in light of the Paris Agreement (2016) for CO_2 emissions cuts, and construction and design advantages. One of the limitations that hinders the use of engineered timber at greater scale is the establishment of robust and rigid timber connections that can transfer high tensile axial loads and limit lateral story drifts. Glued-in rod connections are a suitable candidate for these applications due to their high axial stiffness and load transition, superior fire performance and ease of installation. The use of

[1]Definition of a tall timber building based on Foster et al. (2016)

composite materials such as carbon fibre reinforced polymer (CFRP) and glass fibre reinforced polymer (GFRP) rods can result in improved durability for these connections under high moisture contents (e.g. Service Class 3 (EC5 2004)- Relative Humidity of the surrounding air exceeding 85% for several weeks per year), lower weight and better chemical compatibility between the resin and the FRP rods. Schematic details for timber diagrid structural systems with glued-in rods connected perpendicular and at an angle to the grain are shown in Figure 1.

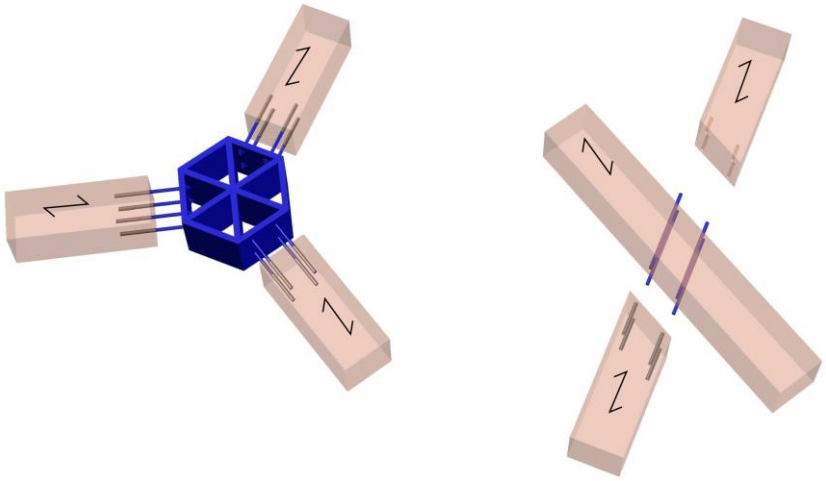

Figure 1: Schematic connection details for diagrid structural systems with glued-in rods.

Existing literature (e.g. Mettem et al. 1999 and Aicher et al. 1999) and applications (Strahm 2000) have emphasised the use of steel rods and limited research has been carried out on the use of FRP (fibre reinforced polymer) rods focusing either on GFRP (Madhoushi & Ansell 2004) or CFRP materials (De Lorenzis et al. 2005). Despite the considerable studies in glued-in steel rods (e.g. GIROD programme), there seems to be no consensus in the establishment of design methods for Eurocode 5. Various authors and national design guidelines relate the bond strength of glued-in steel rods to different parameters (e.g. timber density or glue strength), and experimental results can often be contradictory. Steiger et al. (2006) showed that the bond strength of steel rods glued parallel into the grain direction is directly influenced by the timber density, reporting bond failures by shearing off of a wooden layer at the anchorage. However, this trend was less pronounced in the experimental results by Aicher et al. (1999) with similar bond failure. Other variables such as glue line thickness, anchorage length, rod diameter, bond test methods and the lack of detailed experimental reporting (e.g. type of bond failure and mechanical properties of the glue material) inhibit firm conclusions. An increase

in the glue-line thickness is usually associated with an increase in the axial load resistance (e.g. in glued-in steel rods with a ductile epoxy adhesive in Feligioni et al. 2003 and with epoxy and polyurethane adhesives in Bengtsson & Johansson 2000), but this is highly dependent on the type of applied adhesive. The use of phenol-resorcinol has resulted in decreased bond performance with increasing glue-line thickness attributed to higher shrinkage effects and the application of polyurethane can yield bubbles at the wood/resin interface due to its reaction with the inherent timber moisture. Epoxy adhesives exhibit higher bond strength regardless of glue-line thickness. Yet, standardisation in bond performances of resins can be hindered due to constant advances in resin formulations that are usually proprietary to the manufacturers (Lees et al. 2017). Moreover, different bond test methods can result in different bond strength results and understanding of the different acting stress mechanisms is needed to enable the establishment of testing procedures. Broughton & Hutchinson (2001) showed that a pull-pull test method in timber can yield higher pull-out loads than a pull-compression test irrespective of the glue-line thickness for steel rods bonded in LVL, but these findings contradict existing literature in bond performance of steel and FRP rods in concrete structures with similar test techniques.

The aim of this study is to compare the bond performance of CFRP and GFRP rods in timber blocks under tensile static and cyclic loading and identify the relationship between bond strength and stiffness and cost for different materials. GFRP rods are usually preferred in structural applications due to their lower cost (~ 1/3 of the CFRP cost). However, CFRP rods exhibit greater fatigue and creep resistance and can result in higher bond strength and stiffness due to their greater elastic modulus (Baena et al. 2009). Therefore, they can be more suitable when high strength timber connections are necessary such that their high initial cost can be justified.

2 Experimental Programme

2.1 Materials

Pultruded FRP rods (Sireg, Italy) with the same core rod diameter (D=10 mm), resin matrix (vinylester), fibre content (>65%), and surface deformation (helically wrapped and sand coated) but different fibre type (glass versus carbon) are used in this study. The outer diameter of the rods accounting for the external sand coating layer is D_o=10.7 mm and D_o=11.1 mm for the CFRP and GFRP rods respectively according to ACI 440.3R-12 (ACI 2012) guidelines.

The rods were glued in timber specimens using a two component thixotropic adhesive of epoxy resin and special filler (Sikadur 30). The nominal mechanical properties, as provided by the manufacturers, are summarised in Table 1. The timber specimens derived from a block laminated spruce C24, made in Stora Enso Ybbs (Austria) factory using their CLT process without the cross-laminated elements.

Table 1. Material properties for FRP rods and epoxy glue.

	CFRP (Carbopree)	GFRP (Glasspree)	Epoxy glue (Sikadur 30)
Longitudinal tensile elastic modulus - E_L (MPa)	130000	46000	11200**
Average tensile strength, f_{ru} (MPa)	2450	1000	26*
Elongation at break, ε_{ru} (%)	1.8	1.8	N/A
Average shear strength, f_{vu} (MPa)	N/A	N/A	16*

*Curing conditions: after 7 days at 15°C, **Curing conditions: after 7 days at 23°C

2.2 Specimen Preparation

A 250 mm CFRP/GFRP rod was placed concentrically in a 70 x 70 x 55 mm timber block, parallel to the grain, and was glued with an epoxy layer of varying thickness (t=1.5, 3 and 5 mm). The bonded length was 50 mm corresponding to 5D where D is the core diameter of the rod. To ensure the proper alignment of the FRP rod along the bonded length, acrylic caps were prepared and applied at the loaded end (end closer to the crosshead of the Instron machine where the load is directly applied) and free end (see Figure 2a). The caps were sprayed with a demoulding agent and covered with silicone rubber (Dow Corning) to enable their easy removal after curing of the epoxy glue. The epoxy was cast vertically in the holes and the specimens were left in that position for at least 1 day before the anchorage preparation. Sleeve anchors were used, to ensure a firm grip on the FRP rods considering their inferior mechanical performance in lateral compression. The anchors consisted of black mild steel tubes with an outer diameter D_o=31.75 mm, thickness, t=3.2 mm and length L=80-90 mm and were filled with epoxy (Sikadur 30 or Sikadur 33). The anchors were aligned horizontally based on the rig shown in Figure 2b. Two types of anchors (Type I and Type II) were used and Type I was preferred to accelerate the alignment procedure. The specimens with a glue-line thickness t=1.5 and 3.0 mm were stored in the lab at T=21.5 ± 3.2°C (standard deviation-STDV) and RH=51.1 ± 7.8% (STDV) and the specimens with a glue-line thickness t=5.0 mm were stored

at T= 22.0 ± 2.3°C (STDV) and RH=53 ± 5.2% (STDV). The specimens are identified here as a-b-c, where 'a' denotes the fibre type (C: Carbon and G:Glass), 'b' denotes the glue-line thickness and 'c' denotes the type of loading (s:static and c:cyclic).

To understand the bond stress transfer mechanism during pulling-out of the rod, one specimen each from the groups C-3.0-s, G-3.0-s, C-5.0-s and G-5.0-s was prepared with 4 strain gauges attached on the surface of the rod and equally distributed over the bonded length. The strain gauge cables were guided through drilled holes of 8 mm diameter from one of the 4 sides of the timber block. To enable the attachment of the strain gauges, the sand coating layer of the FRP rods was removed with a blade along the bonded length for roughly a 5 mm wide surface area.

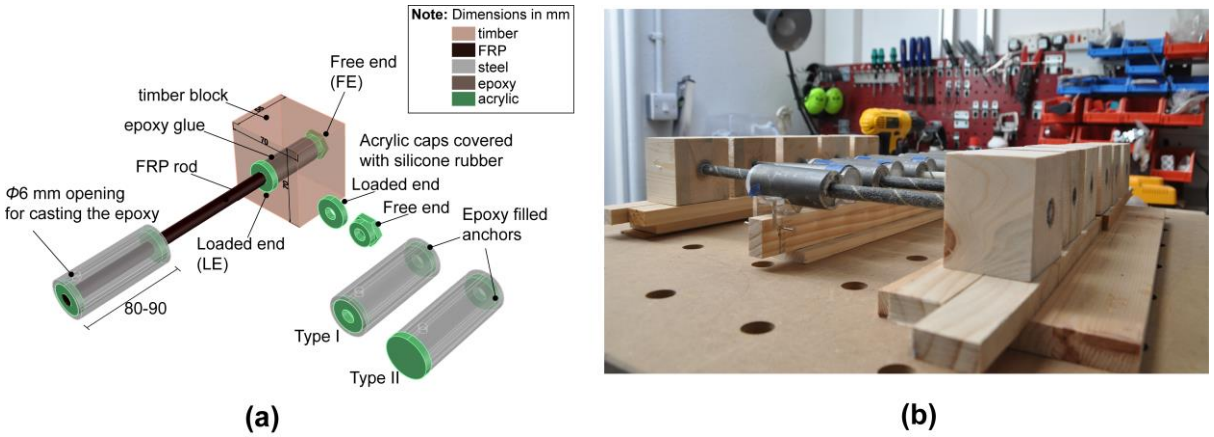

Figure 2. (a) Pull-out test specimen and (b) Alignment rig for the anchorage preparation.

2.3 Test Method

To measure the bond strength of the FRP rods glued in timber blocks, the pull-compression test method (or defined elsewhere as pull-out test) was selected due to its simplicity and ease of application for mechanical screening. The FRP rods were pulled out from the timber block that reacted against a fixed steel plate (see Figures 3a and 3b).

All specimens were tested after at least 10 days of curing of the epoxy glue. The tests were carried out in an Instron machine with a 150 kN load cell capacity in displacement control. Five specimens from each of the 12 groups (60 samples in total) were tested in a static and cyclic loading regime at a displacement rate of 0.5 mm/min. The cycling regime consisted of 3 load-unload repetitions at three target loads of 0.20-0.25F_{us}, 0.4-0.5F_{us} and 0.60-0.75F_{us}, where F_{us} is the average

pull-out failure load of each group tested statically, followed by loading up to failure. Slip values were recorded with 2 LVDTs (Linear Variable Differential Transformers) at the loaded end and 1 LVDT at the free end. Any displacement of the steel reaction plate was recorded with an LVDT during testing. Strain gauges were attached selectively at the loaded end of 4 GFRP and CFRP rods to measure experimentally their longitudinal elastic Young's modulus during the pull-compression test method. The slip values at the loaded end were corrected for the rod extension and the plate displacement and therefore the differences in the elastic modulus between the CFRP and GFRP rods were not considered. The rod extension was calculated based on the experimental elastic Young's moduli values, that were 19% and 36% higher than the nominal values of the CFRP and GFRP rods respectively, and the free unbonded length of the rod between the two anchorage points (the anchor and the loaded end). The corrected slip values were considered to be more representative of a glued in rod connection between two timber structural elements, where the unbonded length is negligible.

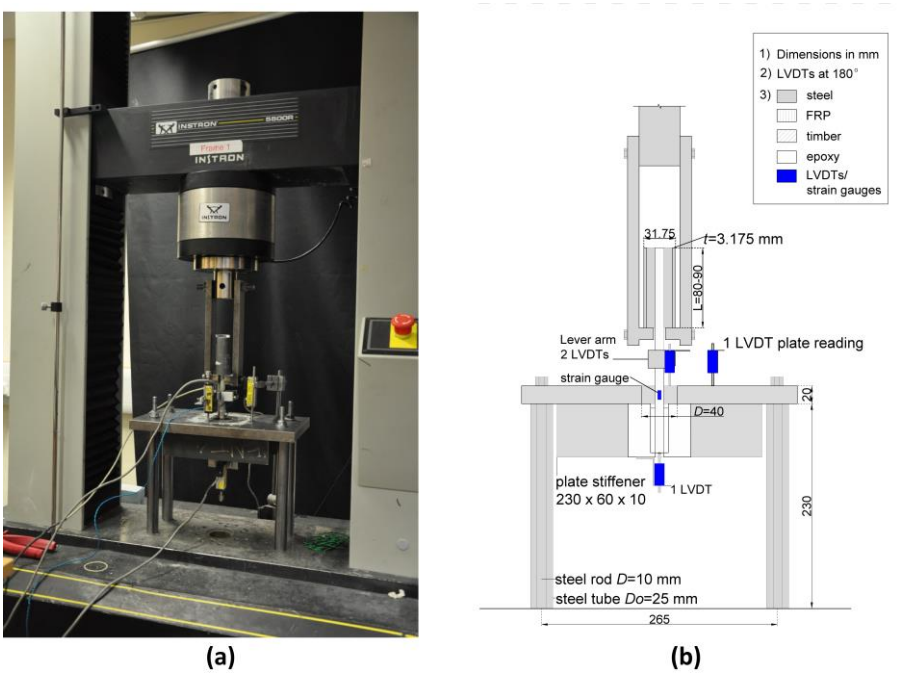

Figure 3. Pull-out test set up, (a) Photo of actual test set up and (b) Drawing.

3 Results and Discussion

3.1 Bond strength

Figure 4a shows the average pull-out load values, F_u, for each glue-line thickness (t=1.5, 3.0 and 5.0) and each rod material (CFRP and GFRP) after static and cyclic loading. Figure 4b shows the average bond strength values as derived

from the failure pull-out loads normalised by the surface area of the drilled hole diameter in timber, assuming a uniform bond stress distribution over the bonded length. The hole surface area was adopted as a reference area since most bond failure mechanisms occurred in the wood/resin interface. The error bars indicate one standard deviation. The red dots represent the specimens with the 4 strain gauges over the bonded length that were tested statically. These specimens were excluded from the group's average values, because it was assumed that the occupied volume of the cables from the strain gauges would result in discounted bond performance. All specimens had a timber moisture content of 9.3 ± 0.7 % (STDV) as measured with a moisture meter (EXTECH M0220) after testing.

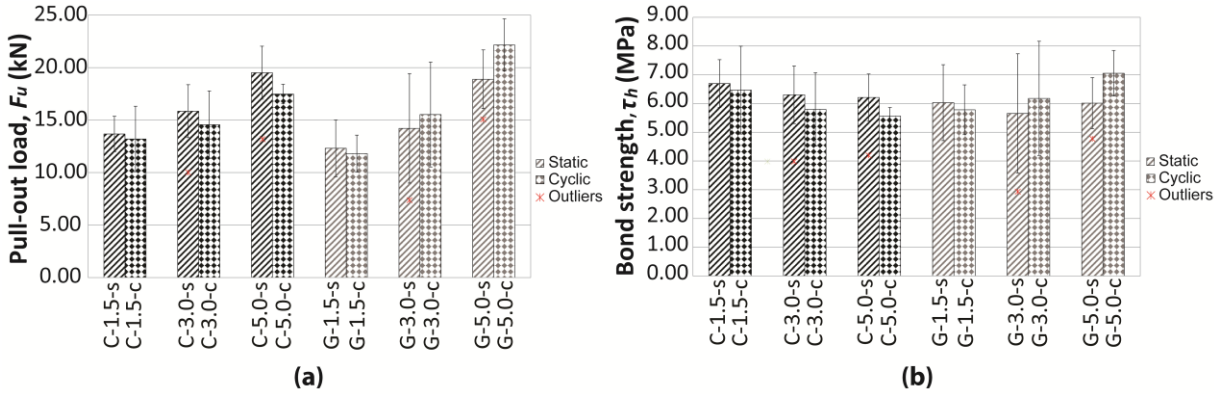

Figure 4. (a) Failure pull-out load and (b) Bond strength values after static and cyclic loading for glued-in CFRP and GFRP rod connections in timber.

All rods (CFRP and GFRP) showed an increasing trend in the average pull-out load with an increase in the glue-line thickness. Rises up to 43 and 53% were recorded under static loading with a 3.5 mm increase in the glue-line thickness for CFRP and GFRP rods respectively. Different trends were observed in terms of normalised load and bond strength values, as shown in Figure 4b. CFRP rods showed a 7% decrease in the bond strength by comparing the C-1.5-s with the C-5.0-s group and GFRP rods showed a negligible difference for the same glue-line thickness variations. In conclusion, failure loads, bond strength values and reference surface areas should be highlighted in each study in glued-in rod connections to avoid misinterpretations.

CFRP rods exhibited consistently higher average pull-out loads than the GFRP rods under static loading irrespective of the glue-line thickness. The difference between the two materials was more dominant at smaller glue-line thickness (t=1.5, 3.0 mm) where CFRP rods showed 11% higher axial load resistance. The cyclic loading seems to deteriorate the average axial load resistance of CFRP

rods and a maximum 10% decrease is recorded for a glue-line thickness t=5.0 mm (C-5.0-c versus C-5.0-s). It should be noted that one of the five specimens in group C-1.5-c failed at the first loading of the 3rd cycle (0.66F_{us}) at 8.09 kN. Under cyclic loading GFRP rods seemed to perform better and yielded the maximum average axial load resistance among the groups, F_u=22.16 kN, for a glue-line thickness t=5.0 mm. However, considering the observed standard deviations in the bond strength of the glued-in CFRP and GFRP rods in timber and the material variability, it can be inferred that cyclic loading does not affect the bond strength. The experimental findings agree with the existing literature. Indicatively, the G-1.5-s group yielded an average pull-out load of F_u=12.32 kN and Mettem et al. (1999) has reported an average pull-out load of F_u=12.2 kN for GFRP rods with a diameter D=8.0 mm glued into LVL with a 2 mm epoxy glue-line thickness and a 60 mm bonded length. The experimental results suggest that the increase in the pull-out load and the hole surface area are linearly related for both types of rods but an approximately six times increase in the glue volume can lead to a rise in axial load resistance of up to 88% (G-5.0-c versus G-1.5-c). Therefore, the relevant benefits in the axial load resistance from an increase in the glue volume and consequently cost should be estimated using engineering judgement.

3.2 Bond stress-slip plots

The bond stress-slip plots for the CFRP rods under cyclic loading are depicted in Figure 5 for the different glue-line thicknesses studied. The slip values refer to the loaded end. It can be observed that there is no decrease in the gradient and thus the stiffness of the glued-in rod connections upon cyclic loading. An increase in the residual slip values after unloading is detected and it is more pronounced with increasing loading and glue-line thickness. This is attributed to cyclic creep that is representative of viscoelastic materials such as timber and epoxy resins. The failure of the CFRP rods glued in timber parallel to the grain was brittle with a sudden drop in bond strength up to 94% of the peak values (see Figure 5d). GFRP rods exhibited similar performance.

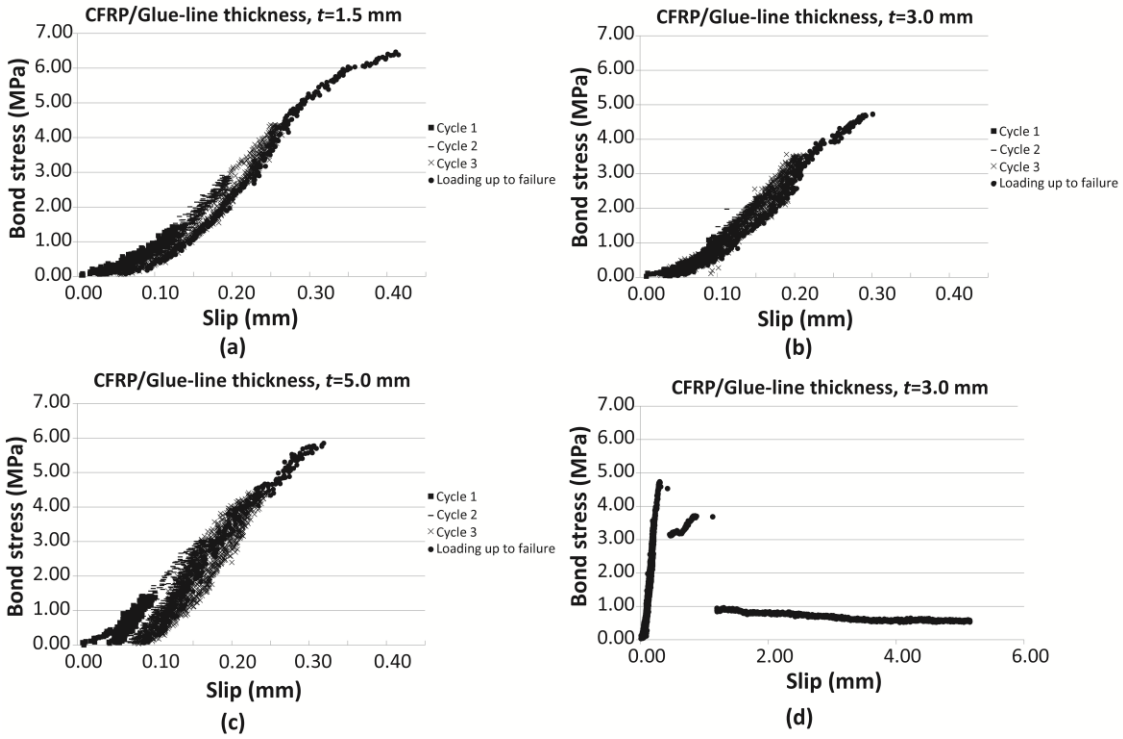

Figure 5. Bond stress-slip plots at cyclic loading for a CFRP rod with (a) glue-line thickness, t=1.5 mm, (b) glue-line thickness, t=3.0 mm, (c) glue-line thickness, t=5.0 mm and (d) after post-failure for glue-line thickness, t=3.0 mm.

3.3 Secant stiffness

Figures 6a and 6b depict the secant stiffness derived from the pull-out load versus slip plots at the Ultimate Limit State (ULS) and Serviceability Limit State (SLS). The Serviceability limit state was defined between 10 and 40% of the ultimate failure load, F_u, where structures are mostly expected to be loaded during their design life and to align with the slip modulus definition, K_{ser}, for steel dowel connections. At cyclic loading the secant stiffness was calculated as the ratio of the failure load to the loaded end slip value corrected for any residual slip at zero load. The secant stiffness at both ULS and SLS exhibited high values for a glue-line thickness of t=5.0 mm under both static and cyclic loading. Most specimens had a higher secant stiffness after cyclic loading with maximum values of K_{SLS}= 99.7 kN/mm, K_{SLS}=189.1 kN/mm and K_{ULS}=91.8 kN/mm and K_{ULS}= 106.8 kN/mm for the groups C-5.0-c and G-5.0-c respectively. This was attributed to the stiffer response observed with increasing loading combined with the corrected slip values for the residual deformations. The difference in the stiffness between glue-line thicknesses t=1.5 and 3.0 were limited to around +/- 18% at both static and cyclic loading except that the G-3.0-s group showed 43% lower stiffness at ULS and the C-3.0-s showed 35% lower stiffness at SLS. The slip modulus of a single dowel connection with a 10 mm steel dowel for the same timber grade is 3.7 kN/mm per shear plane according to Eurocode 5 and

can vary up to 14.8 kN/mm accounting for two shear planes and a steel-to-timber connection. However, a higher stiffness up to 38.4 kN/mm has been experimentally reported by Reynolds et al. (2016) for a single dowel connection with a 12 mm steel dowel in C16 Sitka spruce.

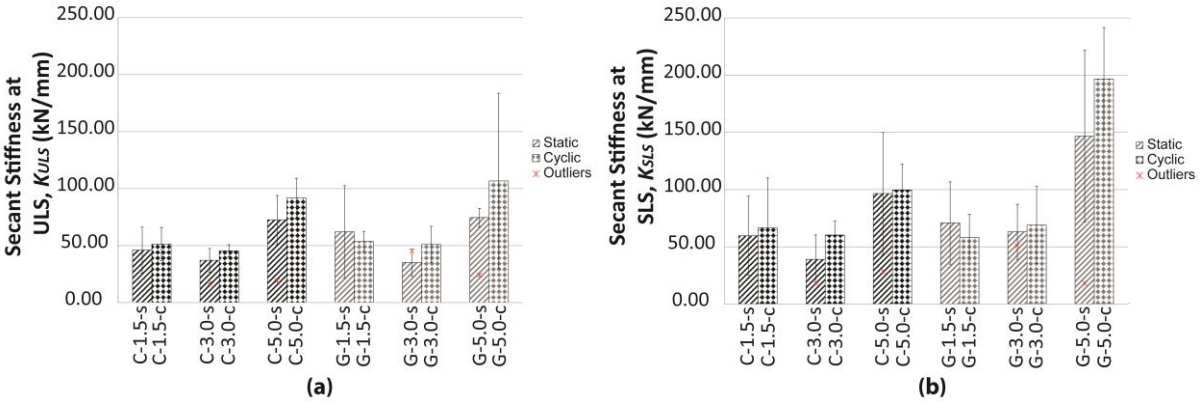

Figure 6. Secant stiffness for glued-in CFRP and GFRP rods in timber at (a) Ultimate limit state (ULS) and (b) Serviceability Limit State (SLS).

3.4 Bond failure mechanisms

The majority of the specimens failed at the wood/resin interface (W/R) (see Figure 7d) followed in some cases by a wood plug failure (WP). Mixed-mode bond failure was also observed, such as wood/resin (W/R) combined with resin/FRP (R/F) interface failure and wood/plug with resin/FRP interface failure. The definition of the bond failure mechanisms adopted in this study is depicted in Figure 7c. In the resin/FRP failure mode the failed interface was mostly between the external sand coating layer and the core rod indicating a good adhesion between the glue and the FRP. In Figures 7a and 7b the failure mechanisms with respect to the glue-line thickness and the experimental pull-out load are classified for the clear and mixed-mode bond failures. The highest axial load resistance is observed for resin/FRP interface failure modes at a glue-line thickness of t=5.0 mm. Considerable variations in the pull-out load lie among the W/R failure modes and firm conclusions cannot be derived. Splitting failures seem not to be linked with lower failure loads, but this can depend on the adopted test method (pull-compression).

In 15 specimens out of the 60 tested in total, the wood plug failure extended up to the hole of the reaction plate. This was mostly observed in the groups C-1.5-s and C-1.5-d. This type of failure might not have been observed in a pull-pull test procedure indicating that the bond test method can affect the bond failure and

possibly the recorded experimental bond strength values. In the wood plug failure the failed surface propagated along the growth rings at the latewood/earlywood interface or within the earlywood, as schematically shown in Figure 7c(i). During pulling out, shear stresses develop at the interface between earlywood and latewood due to the inherent differences in density and thus stiffness between the adjacent growth rings. In some specimens the wood plug failure was limited to one lamina of the timber block and the crack pattern did not expand to the adjacent one. Therefore, the wood plug failure mechanism and the relevant bond strength values are more related with the timber density (as suggested by Steiger et al. (2006)), compared with the wood/resin and resin/FRP failure mechanism. Variations in the bond strength due to material variations are also expected. By observing the wood plug failure pattern, the peak failure load seems to be related to the wood shear strength in both the longitudinal/radial and longitudinal/tangential plane. Noises of imminent failure followed with occasional visually detected radial cracks were observed during the cyclic loading at $0.75F_{us}$. Splitting was associated with 18 bond failure mechanisms (see Figures 7a and 7b) and it was mostly observed in specimens with a thicker glue-line (t=3.0 and t=5.0 mm). Splitting cracks propagated along the growth rings, were restricted in some cases within the lamina and they usually developed in the vicinity of a knot as observed in the face/edge grain of the specimen. More splitting failures were observed in GFRP rods at a glue-line thickness of t=1.5 mm and t=3.0 mm and for CFRP rods this was dominant at a glue-line thickness of t=5.0 mm. A higher number of splitting bond failure modes have also been recorded for Near Surface Mounted GFRP ribbed rods used in normal strength concrete when a smaller groove size and thus epoxy layer thickness was applied (De Lorenzis et al. (2002)). Similar CFRP ribbed rods but with less pronounced ribs exhibited failure at the epoxy-concrete interface. A greater splitting tendancy has also been observed by Achillides & Pilakoutas (2002) in GFRP bars used as a reinforcement in concrete beams and when an adequate concrete cover was not provided. This was attributed to the lower Elastic modulus of the GFRP bars that affects their deformability both in the longitudinal and transverse direction (Poisson's ratio effect). Nevertheless, the Poisson's ratio effect should result in tensile stresses in the radial direction, where the splitting crack and radial cracks develop, based on a thick walled analysis as previously used by Tepfers (1979). De Lorenzis et al. (2005) showed that the splitting bond strength depends on the depth of the provided cover when FRP rods are glued in timber parallel to the grain by adopting a thick walled analysis. However, this analytical approach is valid for isotropic materials and might not be suitable for anisotropic materials like timber. Madhoushi & Ansell (2017) showed that the increase in glue-line

thickness for GFRP rods alleviates the axial stress concentration along the glue lines by carrying out a FE analysis. In conclusion, further investigation is needed to comprehend the effect of the glue-line thickness and the interaction of the glue and FRP (due to their inherent different material properties) in the axial stress distribution at the end grain and in the bond shear stress distribution along the bonded length.

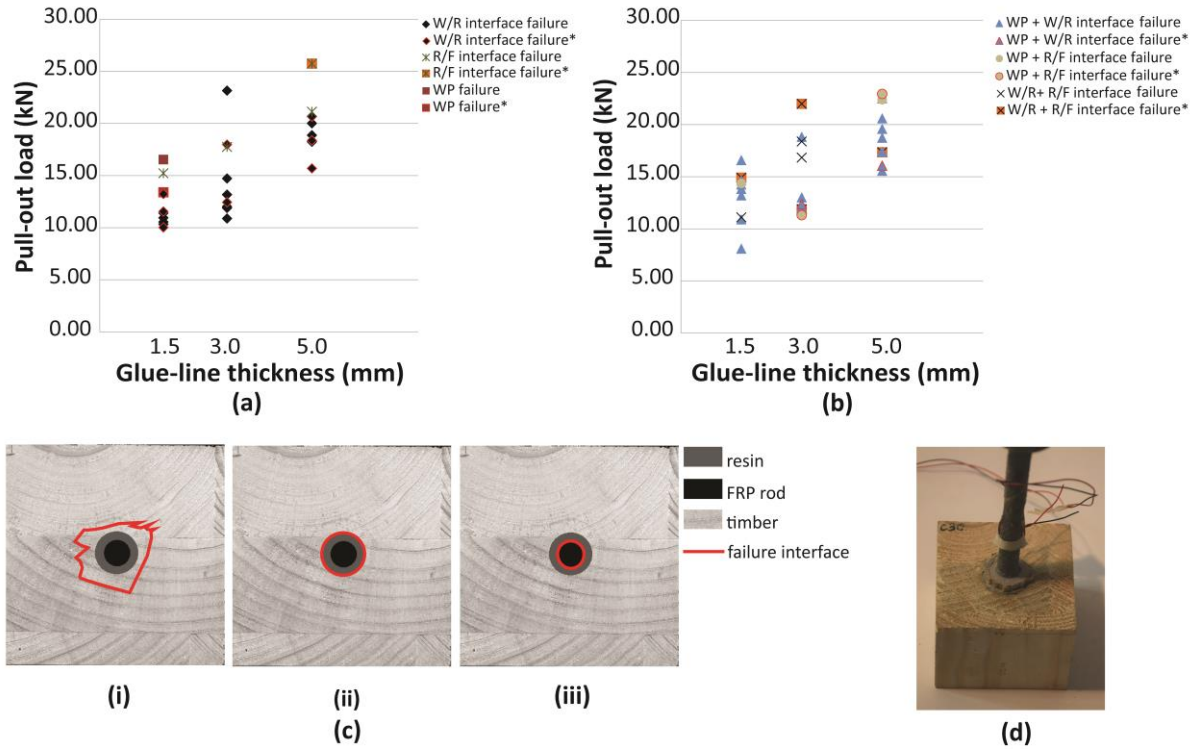

*Figure 7. Pull-out load versus glue-line thickness for (a) clear bond failure mechanisms and (b) mixed-mode bond failure mechanisms, (c) Definition of bond failure mechanisms-schematic, (i) wood plug failure, (ii) wood/resin interface failure and (iii) resin/FRP failure and (d) actual photo of a typical wood/resin interface failure. Note: WP: wood plug failure, W/R: wood/resin interface failure, R/F: resin/FRP interface failure and * denotes splitting failure.*

3.5 Axial strain distribution

Figures 8a and 8b depict the axial strain distribution along the bonded length for a specimen tested statically with a CFRP and GFRP rod respectively and a glue-line thickness of 5.0 mm.

In the plots the loaded and free end correspond to x=5.0 mm and x=47.0 mm respectively, where x is the centre to centre distance of the strain gauges along the bonded length. A linear strain distribution is observed for both FRP rods up to 25% of their failure load indicative of a uniform bond stress distribution. At higher loads similar strain readings are recorded at the vicinity of the loaded

end suggesting that a local debonding failure takes place. At the failure load the maximum strain values are derived at a distance, *x*=19 mm, followed by a linear strain distribution. A deviation from a linear strain distribution is observed in the CFRP rod at *x*=33.0 mm. Inspection of the specimen by splitting it open after testing showed a local void at this location for roughly ¼ of the rod surface area impeding a full wood/resin contact. The specimen with the GFRP rod had a full wood/resin contact along the bonded length. The uniform bond stress assumption seems not to be valid for bonded lengths greater than or equal to 5 times the rod diameter at a glue-line thickness of 5.0 mm due to the local debonding observed. The method adopted with the 4 strain gauges along the bonded length seemed inefficient for the 3.0 mm glue-line thickness. The strain readings were inconsistent between FRP rods and inspection of the specimens showed unbonded areas up to half the surface of the rod. This was the result of the occupied space from the cables of the strain gauges in combination with the thixotropic nature of the epoxy.

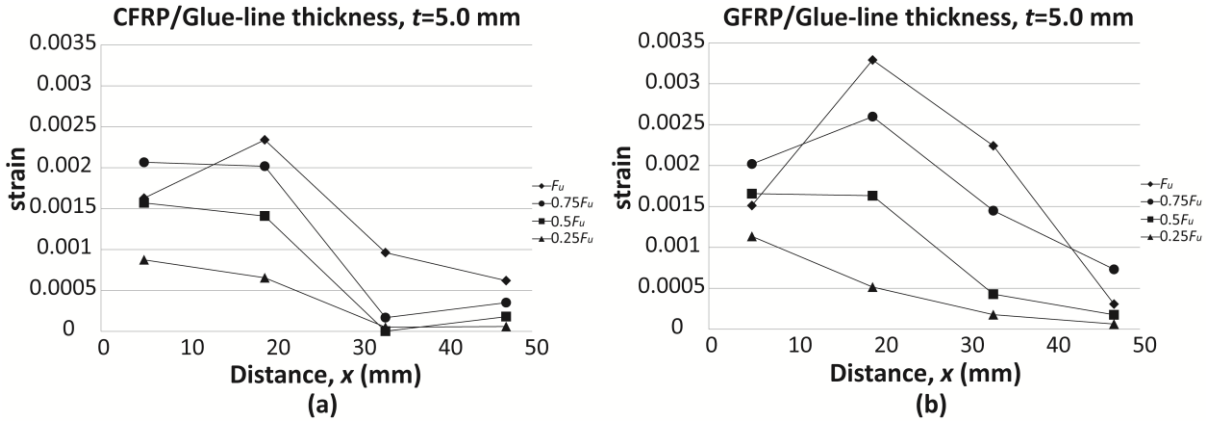

Figure 8: Axial strain distribution for (a) a CFRP rod and (b) for a GFRP rods glued –in timber with a glue-line thickness of t=5.0 mm.

4 Conclusions

CFRP rods exhibit a higher bond performance under static loading up to 11% compared with GFRP rods but GFRP rods yield higher bond stiffness at SLS, K_{SLS} under the same loading regime (up to 90%). Given the considerable difference in cost between the two materials, GFRP rods seem to be the optimum solution for glued-in FRP rod connections in timber. However, the long-term performance of glued-in GFRP and CFRP rods in timber (e.g. under fatigue and sustained loading) should be also investigated in the future to derive firm conclusions. The increase in the glue-line thickness increases significantly the

average axial load resistance but this is reflected in a much higher use of glue epoxy and consequently cost.

5 Acknowledgements

The presented work is supported by a Leverhulme Trust Programme Grant. The timber material was provided by Stora Enso.

6 References

Achillides, Z. and Pilakoutas, K. (2002): Analytical approach to the bond behaviour of FRP bars in concrete. Proc., Int. Symp. on Bond in Concrete from Research to Standards, G.L. Balázs, P.J.M. Bartos, J. Cairns and A. Borosnyói eds., Budapest University of Technology and Economics, Hungary, 700-707.

ACI 440.3R-12 (2012): Guide Test Methods for Fiber-Reinforced Polymers (FRPs) for Reinforcing or Strengthening Concrete Structures. American Concrete Institute, Farmington Hills, MI, USA.

Aicher, S., Gustafsson, P.J. and Wolf, M. (1999): Load displacement and bond strength of glued-in rods in timber influenced by adhesive, wood density, rod slenderness and diameter. In Proceedings of 1st RILEM Symposium on Timber Engineering, 369-378.

Baena, M., Torres, L., Turon, A., and Barris, C. (2009): Experimental study of bond behaviour between concrete and FRP bars using pull out test. Composites: Part B, 40(8), 784-797.

Bengtsson, C. and Johansson, C.J. (2000): Test methods for glued-in rods for timber structures. Paper 33-7-8. In: Proceedings of the 33th conference of CIB-W18, Delft, Netherlands.

Bengtsson, C. and Johansson, C.J. (2002): GIROD-glued-in rods for timber structures: Final report. SMT4-CT97-2199.

Broughton, J.G. and Hutchinson, A.R. (2001): Pull-out behaviour of steel rods bonded into timber. Materials and Structures, 34, 100-109.

BS EN 1995 Eurocode 5 (2004): Design of timber structures - Part 1-1: General - Common rules and rules for buildings.

De Lorenzis, L., Rizzo, A. and La Tegola, A. (2002): A modified pull-out test for bond of near-surface mounted FRP rods in concrete. Composites Part B: Engineering, 33(8), 589-603.

De Lorenzis L., Scialpi, V. and La Tegola, A. (2005): Analytical and experimental study on bonded-in CFRP bars in glulam timber. Composites Part B, 36(4), 279-289.

Feligioni, L., Lavisci, P., Duchanois, G., De Ciechi, M. and Spinelli, P. (2003): Influence of glue rheology and joint thickness on the strength of bonded-in rods, Holz als Roh- und Werkstoff, 61(4), 281-287.

Foster, R.M., Reynolds, T.P.S. and Ramage, M.H. (2016): Proposal for Defining a Tall Timber Building, Journal of Structural Engineering, 142(12).

Lees, J.M., Toumpanaki, E., Barbezat, M. and Terrasi, G.P. (2017): Mechanical and Durability Screening Test Methods for Cylindrical CFRP Prestressing Tendons, Journal of Composites for Construction, 21(2).

Madhoushi, M. and Ansell M.P. (2004): Experimental study of static and fatigue strengths of pultruded GFRP rods bonded in LVL and glulam. International Journal of Adhesion and Adhesives, 24(4), 319-325.

Madhoushi, M. and Ansell, M.P. (2017). Effect of glue line thickness on pull-out behaviour of glued in GFRP rods in LVL: Finite element analysis. Polymer Testing, 62(2017), 196-202.

Mettem, C.J., Harvey, K. and Broughton, J.G. (1999): Evaluation of material combinations for bonded in rods to achieve improved timber connections. In CIB-W18, Meeting 32, Graz, Austria, 1-14.

Reynolds, T., Sharma, B., Harries, K. and Ramage, M. (2016): Dowelled structural connections in laminated bamboo and timber. Composites Part B, 90(2016),232-240.

Sanner, J., Snapp, T., Fernandez, A., Weihing, D., Foster, R. and Ramage, M. (2017): River Beech Tower: A Tall Timber Experiment. CTBUH Journal, Issue II, 40-44.

Steiger, R., Gehri., E. and Widmann, R. (2006): Pull-out strength of axially loaded steel rods bonded in glulam parallel to the grain. Materials and Structures, 40, 69-78.

Strahm, T. (2000): The GSA-system of anchorage: efficient and easy to design. Proceedings of the 32 SAHFortbildungskurs “Verbindungstechnik im Holzbau, Weinfelden, Switzerland, 165–169 (only available in German)

Tepfers, R. (1979): Cracking of concrete cover along anchored deformed reinforcing bars. Magazine of Concrete Research, 31(106), 3-12.